

MRCI Calculation, Scaling of the External Correlation, and Modeling of Potential Energy Curves for HCl and OCl

A. Peña-Gallego, P. E. Abreu, and A. J. C. Varandas*

Departamento de Química, Universidade de Coimbra, P-3049 Coimbra Codex, Portugal

Received: November 15, 1999; In Final Form: April 6, 2000

The first lowest ${}^2\Pi$ and ${}^2\Sigma^+$ states of OCl, as well as the ${}^1\Sigma^+$ and ${}^3\Sigma^+$ states of HCl, have been calculated at the ab initio MRCI level, and modeled semiempirically using the extended Hartree–Fock approximate correlation energy method. Spectroscopic RKR data and accurate ab initio energies have been used to obtain the model parameters. The vibrational levels of those states have also been calculated, and found to be in good agreement with existing spectroscopic data for the ground electronic states of the title diatomic molecules.

1. Introduction

Hypochlorous acid^{1–3} (HOCl) plays an important role in the ozone layer depletion, with the diatomic species OCl, OH, and HCl also taking part in this process. It comes therefore as no surprise that it has been and continues to be much investigated, both experimentally^{4–6} and theoretically.^{7–10}

For a description of the involved chemical reactions, such as predissociation and photodissociation processes and other energy transfer phenomena, it is essential to have an accurate representation of the relevant HOCl potential energy surfaces as a function of the internal coordinates. Experimentally, a direct Rydberg–Klein–Rees (RKR)^{11,12} inversion of vibrational–rotational spectroscopic data to get the potential function is feasible only for diatomic molecules. For larger polyatomics, the procedure is more complicated and usually requires a trial-and-error approach. This starts with a model potential energy surface containing adjustable parameters which are then optimized through a comparison of the calculated and measured properties.

For chemically stable diatomic molecules, and in some cases also for less stable ones of the van der Waals type, accurate potential energy curves can be obtained by using the RKR method. However, RKR potentials are given in tabular form, and defined only for regions of the potential energy curve covered by the spectroscopic data (i.e., over the attractive regions of the potential curve). Thus, for molecular dynamics studies, it is most convenient to have an analytic form which accurately reproduces the RKR data and extends it to the inner repulsive and long-range attractive regions of the potential energy curve where such data is missing. Of course, the RKR turning points offer whenever available an accurate reference standard for testing the ab initio electronic structure calculations which can provide molecular energies at any point of the molecule configuration space. However, as for the RKR method, such energies are given in tabular form. In addition, ab initio molecular orbital methods present computational difficulties at large interatomic distances where weak long-range forces play a dominant role. At such regions, long-range perturbation theory would be best suited, but the results would then not be valid at the short-range part of the potential curve where charge overlap and electron exchange effects become important. Obviously, such difficulties are compounded as the number of atoms in the polyatomic molecule increases. In summary, despite con-

siderable progress in recent years, ab initio potential energy surfaces which reproduce all the data to the observed experimental accuracy are few and far between.

To avoid the above difficulties, it has been suggested to use semiempirical potential models containing a few adjustable parameters which are determined from a fit to reliable theoretical and/or experimental data. One such successful model which we employ in the present work involves the partitioning of the total energy into an extended Hartree–Fock type (EHF) energy, which includes the so-called nondynamical or internal correlation, and a dynamical or external correlation part^{13,14} which contains the long-range dispersion energy at the separated fragments limit. The nondynamical correlation energy can in principle be modeled from accurate ab initio calculations (which are currently feasible at this level of theory for most diatomic molecules and also larger polyatomics) or available spectroscopic data, while the dynamical correlation is approximated semiempirically from data referring to the interacting fragments (e.g., atomic polarizabilities in the case of a diatomic molecule). The method has been named EHFACE2,¹⁵ the acronym for extended Hartree–Fock approximate correlation energy, with the digit standing for diatomics. Note that without having to sacrifice too much simplicity, this model has been extended to cover the highly repulsive regions of the potential curve near the limit for the collapsed diatomic molecule ($R \rightarrow 0$) by taking into account the normalization of the kinetic field.¹⁶ It has then been named EHFACE2U,¹⁷ where U stands for the united-atom limit. The EHFACE2(U)^{15–17} models can therefore provide an accurate description of the whole potential energy curve, including the asymptotic limits $R \rightarrow 0$ and $R \rightarrow \infty$.

A major goal of the current work is to obtain EHFACE2(U)-type potentials for the diatomics involved in the photodissociation process of HOCl: OCl in both the ground (${}^2\Pi$) and excited $A^2\Sigma^+$ electronic states, and HCl in the ground (${}^1\Sigma^+$) and excited $A^3\Sigma^+$ states. Since the involved HO potentials have been reported elsewhere,¹⁸ no further reference to them will be made here. Thus, we report accurate ab initio calculations of four different potential energy curves, by employing a large basis set and MRCI^{19,20} methods which take as reference a full valence complete active space^{21,22} (FVCAS) wave function. The calculated MRCI energies are then corrected by scaling the external correlation energy within the spirit of the SEC^{23,24} method. Finally, EHFACE2(U)-type potentials are modeled either by

fitting available experimental RKR turning points or the calculated SEC energies.

The paper is organized as follows. In Section 2, we provide a description of the EHFACE2(U) models. The ab initio calculations and the main features of the SEC method are given in Section 3. Section 4 reports the calculated EHFACE2(U) potential energy curves, and compares them with the available experimental and theoretical data. The concluding remarks are in Section 5.

2. Method

In the EHFACE2 method, the potential energy is written as

$$V = V_{\text{EHF}}(R) + V_{\text{dc}}(R) \quad (1)$$

where EHF denotes the extended Hartree–Fock type energy, and dc the dynamical correlation which includes the asymptotic long-range dispersion energy. As usual, we maintain the designation V_{dc} even when this term accounts also for the long-range electrostatic and induction energies, which appear in the EHF part of the interaction energy.

The EHF part of the potential assumes the form,¹⁷

$$V_{\text{EHF}} = -DR^{-1} \left(1 + \sum_{i=1}^3 a_i r^i \right) \exp[-\gamma(r)r] \quad (2)$$

where

$$\gamma = \gamma_0 [1 + \gamma_1 \tanh(\gamma_2 r)] \quad (3)$$

In this equation, $r = R - R_e$ is the displacement coordinate from the equilibrium geometry R_e , and D , γ_i , and a_i ($i = 1-3$) are parameters to be determined from a least-squares fit to ab initio or experimental data.¹⁷ For simplicity, no attempt is made to reproduce the correct behavior of the asymptotic exchange energy (ref 18, and references therein). This appears justified for consistency reasons given the approximations involved in scaling the external correlation of the excited-state curves.

In turn, the dynamical correlation energy is approximated by^{25,26}

$$V_{\text{dc}} = - \sum_n C_n \chi_n(R) R^{-n} \quad (4)$$

where the damping functions for the dispersion coefficients are defined by

$$\chi_n(R) = [1 - \exp(-A_n R/\rho - B_n R^2/\rho^2)]^n \quad (5)$$

and the auxiliary functions A_n and B_n assume the form

$$A_n = \alpha_0 n^{-\alpha_1} \quad (6)$$

$$B_n = \beta_0 \exp(-\beta_1 n) \quad (7)$$

with α_i and β_i being universal and dimensionless parameters determined from a fit to the ab initio results for $\text{H}_2(b^3\Sigma_u^+)$: $\alpha_0 = 16.366\ 06$, $\alpha_1 = 0.701\ 72$, $\beta_0 = 17.193\ 38$, and $\beta_1 = 0.095\ 74$. Moreover, ρ is a scaling distance defined (in atomic units) by $\rho = (5.5 + 1.25R_0)$, where $R_0 = 2(\langle r_X^2 \rangle^{1/2} + \langle r_Y^2 \rangle^{1/2})$ is the Le Roy parameter²⁷ and $\langle r_X^2 \rangle$ is the expectation value of the squared radii for the outermost electrons in atom X (similarly for atom Y). To obtain the values of the C_8 and C_{10} dispersion coefficients, we have employed the universal correlation¹³

$$C_n/C_6 = \kappa_n R_0^{a(n-2)/2} \quad (8)$$

where $\kappa_8 = 1$, $\kappa_{10} = 1.31$, and $a = 1.54$ are universal parameters. All expectation values necessary to evaluate R_0 have been taken from the tabulations of Bunge et al.²⁸ In turn, the C_6 dispersion coefficients for the title systems have been calculated from those of H_2 , Cl_2 , and O_2 ¹⁷ by using the combination rule²⁹

$$C_6^{\text{XY}} \approx (C_6^{\text{XX}} C_6^{\text{YY}})^{1/2} \quad (9)$$

The numerical values of the calculated dispersion coefficients are reported in Table 1.

For ions or neutral systems with permanent electric multipole moments, one may also need to consider the electrostatic and induction energies. It has been suggested that the corresponding damping functions can be obtained from those originally obtained for the dispersion energy simply by using the appropriate powers of n .^{13,17} This is the procedure followed here to deal with the two electronic states of OCl, since both the $\text{Cl}(^2\text{P})$ and $\text{O}(^3\text{P})$ possess a permanent quadrupole moment. It turns out³⁰ that, for the $\text{X}^2\Pi$, the quadrupole–quadrupole C_5 coefficient vanishes, while for the excited $A^2\Sigma^+$ state it has the value $C_5 = 11.55 E_h a_0^5$. Since the $C_5 R^{-5}$ term is expected to dominate at large interatomic separations, one then expects the $A^2\Sigma^+$ state to be lowest at such interatomic distances.

Often, due to the unavailability of sufficient input data to define the shallow van der Waals minimum in repulsive states, we find it useful to represent the EHF part of their potential energy curves by the generalized screened-Coulomb form^{13,18}

$$V_{\text{EHF}} = D'R^{-1} \exp\left(-\sum_{i=1}^m a_i R^i\right) \quad (10)$$

where the parameters are obtained from the calculated ab initio energies through a linear least-squares fitting procedure of $\ln(-V_{\text{ab initio}} - V_{\text{dc}})$ vs R . Of course, the asymptotic behavior of the EHF curve can no longer be reproduced, since the decay rate is dictated by the highest power of R in the exponential. An alternative is to use¹³

$$V_{\text{EHF}} = \tilde{D}R^{-1} \left(1 + \sum_{i=1}^N \tilde{a}_i R^i \right) \exp(-\tilde{\gamma}R) \quad (11)$$

where the coefficients are obtained from a least-squares fitting procedure to the calculated ab initio energies. In fact, by fixing $\tilde{\gamma} = \gamma_0$, one may impose the asymptotic behavior of V_{EHF} to be equal to that of the ground-state curve, as one might expect. Clearly, depending on the calculated value of D , the cusp behavior in eq 10 or 11 at the united-atom limit may be only approximately satisfied.

3. Ab Initio Calculations

To construct the potential energy curve for the considered states of the HCl and OCl systems ($1^2\Sigma^+$ and $3^2\Sigma^+$ for HCl, and $2^2\Pi$ and $2^2\Sigma^+$ for OCl), ab initio calculations have been carried out at the MRCI^{31,32} level using FVCAS^{33,34} wave functions as a reference. In this study, the aug-cc-pvqz (AVQZ) basis sets of Dunning^{35–37} were employed. They consist of $(6s, 3p, 2d, 1f)/[4s, 3p, 2d, 1f]$ contracted functions augmented by diffuse $(1s, 1p, 1d, 1f)$ orbitals for the hydrogen atom, and $(12s, 6p, 3d, 2f, 1g)/[5s, 4p, 3d, 2f, 1g]$ and $(16s, 11p, 3d, 2f, 1g)/[6s, 5p, 3d, 2f, 1g]$ contracted functions with diffuse $(1s, 1p, 1d, 1f, 1g)$ orbitals for the oxygen and chlorine atoms, respectively. All calculations have

TABLE 1: Values of R_0 , and Long-Range Dispersion Coefficients Used in this Work^{a,b}

system	R_0/a_0	$C_6/E_h a_0^6$	$C_8/E_h a_0^8$	$C_{10}/E_h a_0^{10}$
HCl	7.493528	25.12	558.52	16267.66
OCl	6.840157	38.67	747.10	18908.15

^a These parameters assume the same value for all states of HCl and OCl. ^b For the electrostatic coefficients in the case of OCl, see the text.

been carried out on a DEC Alpha 600 workstation using the MOLPRO³⁸ ab initio package. A total of 56, 32, 42, and 48 geometries have been considered for HCl($^1\Sigma^+$), HCl($^3\Sigma^+$), OCl($^2\Pi$), and OCl($^2\Sigma^+$).

The ab initio energies so obtained were then corrected by scaling the dynamical correlation. Note that the nondynamical correlation is system specific and in this sense nontransferable.^{39–42} It is also geometry specific, and hence nonscaleable.^{24,25} The external correlation can be obtained by including in the CI wave function the various excitations from the FVCAS reference configuration to the virtual orbital space.^{19,39–42} However, convergence of the CI expansion with respect to including high-order excitations is difficult,^{19,20} and most MRCI^{43–46} calculations include only single and double replacements from the FVCAS wave function. Although this procedure may recover a large fraction of the dynamical correlation, such calculations often yield bond energies which may be several kcal mol⁻¹ too low and saddle point heights too high. On the other hand, since the specifically geometry-dependent effects are included in the FVCAS wave function, it is expected that the external correlation will be approximately transferable^{19,39–42} and scaleable.^{23,24} It has therefore been suggested^{23,24} that the missing dynamical correlation due to triple and higher excitations as well as due to the incompleteness of the one-electron basis set can be estimated semiempirically by scaling the external correlation energy which is recovered at the FVCAS-CISD level. Such a scheme has been referred to as the SEC (scaled-external correlation) method, and is based on the assumption that the core correlation effects are geometry independent (for a generalization to polyatomic interactions within the context of a many-body expansion, see ref 24).

According to the SEC method, the total energy is written as^{23,24}

$$E_{\text{SEC}}(\mathbf{R}) = E_{\text{FVCAS}}(\mathbf{R}) + [E_{\text{MRCI}}(\mathbf{R}) - E_{\text{FVCAS}}(\mathbf{R})]/\mathcal{F} \quad (12)$$

with the empirical factor \mathcal{F} being usually defined by

$$\mathcal{F} = \frac{V_{\text{MRCI}} - V_{\text{FVCAS}}}{V_d - V_{\text{FVCAS}}} \quad (13)$$

so as to reproduce the bond energy of the diatomic molecule. Thus, V_d is the experimental dissociation energy of the diatomic, and V_{MRCI} and V_{FVCAS} are the energies calculated at the MRCI and FVCAS levels, respectively. We make the further assumption that the value of \mathcal{F} can be transferred without modification to scale the external correlation of the excited electronic states considered in the present work. Although one may expect to recover different percentages of the dynamical correlation for open and closed shell reference states, it is also true that on average such a single scaling parameter may still be used. Note that the FVCAS calculations for both the ground and excited states include open shell configuration state functions. Moreover, such a use of a single scaling parameter for both the ground and excited diatomic states seems justified by the fact that such states dissociate to the same set of ground-state atoms. Table 2

TABLE 2: Parameters Employed to Correct the Dynamic Correlation in the ab initio Calculations

system	$R_e/\text{\AA}$	V_{FVCAS}/E_h	V_{MRCI}/E_h	V_d/E_h	\mathcal{F}
HCl($^1\Sigma^+$)	1.2746	0.145550	0.166985	0.169745	0.885900
OCl($^2\Pi$)	1.5696	0.0562987	0.0909100	0.103024	0.740739

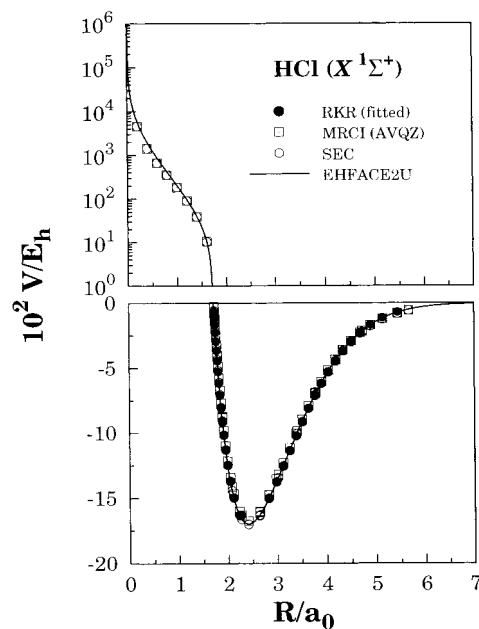


Figure 1. Interatomic potential for HCl($X^1\Sigma^+$). Note that the open circles nearly coincide with the solid ones over the complete range of internuclear distances.

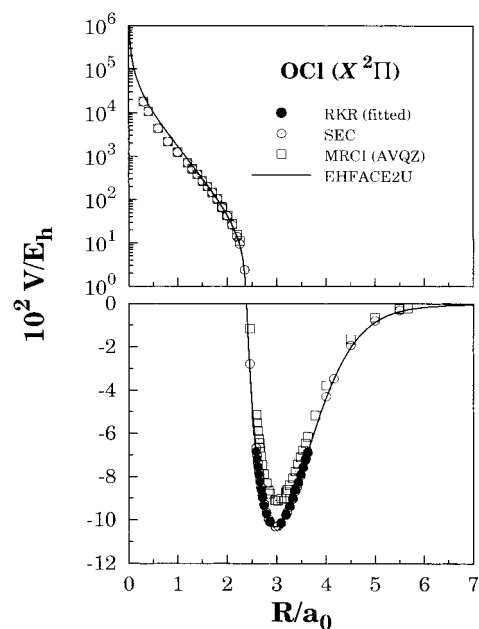


Figure 2. Interatomic potential for OCl($X^2\Pi$). As in Figure 1, the open circles nearly coincide with the solid ones over the regions where they overlap.

gathers the values of \mathcal{F} , and the parameters employed for their calculation.

4. Results and Discussion

Figures 1–4 show the EHFACE2U potential energy curves calculated for the title molecules. We observe that the excited states ($^3\Sigma^+$ for the HCl and $^2\Sigma^+$ for the OCl) considered are repulsive for both molecules, and bound only by weak van der

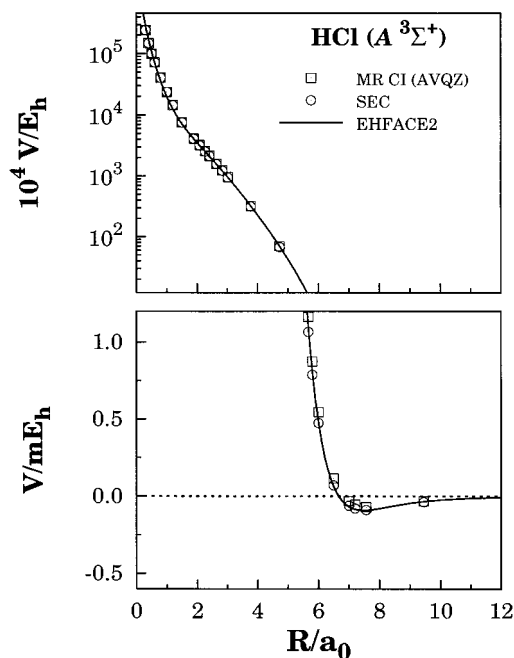


Figure 3. Interatomic potential for HCl($A^3\Sigma^+$).

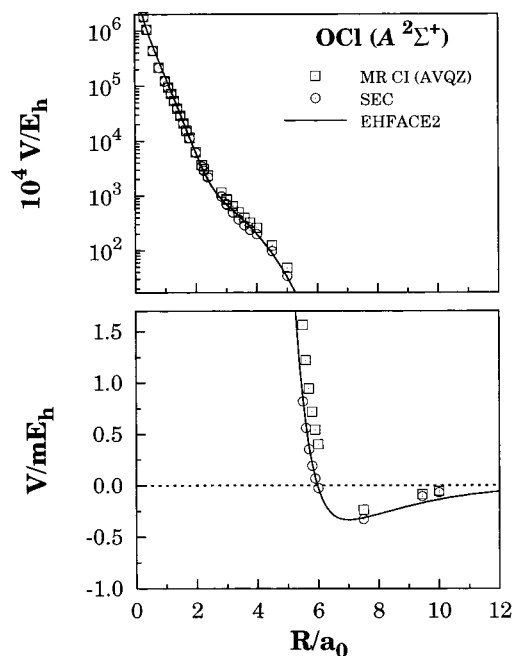


Figure 4. Interatomic potential for OCl($A^2\Sigma^+$).

Waals forces. It is interesting to describe in some detail the fitting procedure which has been used for the various systems.

For the ground states, where RKR turning points are available, these have been employed to obtain the a_i ($i = 1-3$) and γ_i ($i = 0-2$) coefficients, by following method II described in ref 17. This involves a constrained least-squares fitting procedure in which the condition of a normalized kinetic field is imposed. Figure 1 and Figure 2 (for the $^1\Sigma^+$ and $^2\Pi$ states of HCl and OCl, respectively) show that the RKR data is quite accurately fitted in both cases. In addition, it is clear that the curves offer an accurate means to extrapolate the available data to regions not covered by the fitted points. Note that the model has built-in by construction the united-atom and separated-atoms limits. Thus, besides the advantage of warranting a reliable description of the short-range and long-range parts of the potential curve (which may be of use whenever such reliability is requested),

TABLE 3: Values of the Coefficients for the Extended Hartree–Fock Part of the EHFACE2U Potentials

coefficient	HCl		OCl	
	$^1\Sigma^+$	$^3\Sigma^+{}^a$	$^2\Pi$	$^2\Sigma^+{}^b$
$D, \bar{D}/E_h$	0.370 391	18.694 058	0.246 085	61.551 079
$a_1, \bar{a}_1/a_0^{-1}$	1.882 657	-1.160 504	2.498 213	1.377 613
$a_2, \bar{a}_2/a_0^{-2}$	0.745 380	0.716 239	1.466 852	0.240 219
$a_3, \bar{a}_3/a_0^{-3}$	0.307 348	-0.124 454	0.787 479	-1.510 878
\bar{a}_4/a_0^{-4}		0.006 800 24		0.776 447
\bar{a}_5/a_0^{-5}				-0.141 087
\bar{a}_6/a_0^{-6}				0.009 242 53
$\gamma_0, \bar{\gamma}_0/a_0^{-1}$	1.399 596	1.399 596	1.962 760	1.962 760
γ_1	12.067 036		0.517 858	
γ_2/a_0^{-1}	0.008 154 30		0.301 390	

^a $N = 4$ in eq 11. ^b $N = 6$ in eq 11.

the incorporation of information referring to both such asymptotic limits has the merit of transforming the fitting procedure into an interpolation scheme which utilizes the fitted data points to guide the curve at intermediate regions. Clearly, the smooth curves obtained by fitting the experimental RKR points mimic quite well the ab initio points calculated in the present work. Note that the calculated root-mean-square deviations are (in E_h) 0.54×10^{-4} , 2.64×10^{-3} , 0.93×10^{-5} , and 1.48×10^{-3} , respectively for the $^1\Sigma^+$, $^3\Sigma^+$, $^2\Pi$, and $^2\Sigma^+$ states of HCl (first two states) and OCl. For the ground-state curves, this corresponds to 12 cm^{-1} for HCl and 2 cm^{-1} for OCl. The present results corroborate the validity of the SEC approach even for regions quite far away from the equilibrium geometry of the diatomic molecule. The numerical values of the parameters obtained through the calibration process are gathered in Table 3.

To obtain the potential energy curves for the excited states, we have used our own SEC points, since no spectroscopic information seems to be available for such systems. Moreover, we have employed both eqs 10 and 11 to carry out the fits. Yet, for brevity, we give in Table 3 only the numerical parameters obtained by using the latter. Note that the value of D required to reproduce the Coulombic cusp at the united-atom limit should be equal to the product of atomic nuclear charges $Z_X Z_Y$. Clearly, our fitted D values agree only roughly with the theoretical predictions of 17 and 136, respectively for HCl and OCl. Figure 3 and Figure 4 show also that, despite the relatively small number of fitting parameters, the EHFACE2 model provides a good representation of the ab initio data over the whole range of interatomic separations. Note further that no attempt has been made to fit the calculated SEC points in the long-range attractive region of the potential well. Two reasons justify our procedure. First, the fitted SEC energies are based on a scaling factor determined for the ground state curve, and hence are subject to some uncertainty. Second, this region of the potential well is largely dominated by the attractive long-range forces which were defined a priori, and judged adequate.

To test the reliability of the final model potentials, we have carried out calculations of the vibrational levels for the four electronic states of the title diatomic molecules. For this, we have solved numerically the Schrödinger equation for the motion of the nuclei by employing a Numerov–Cooley technique to integrate the wave functions. The results are given in Tables 4–7. Whenever available, we present in these tables the corresponding experimental values for comparison. Clearly, the results obtained for the ground-state curves are in quite good agreement with experiment, with the average deviations being 21 cm^{-1} (0.2%) for HCl and 13 cm^{-1} (0.4%) for OCl. To our

TABLE 4: Vibrational Levels of HCl($^2\Sigma^+$)

v	V/cm^{-1}		$R_{\text{min}}/\text{\AA}$		$R_{\text{max}}/\text{\AA}$	
	calc.	exp.	calc.	exp.	calc.	exp.
0	1466.04	1483.89	1.1768	1.1772	1.3937	1.3934
1	4339.02	4369.87	1.1167	1.1172	1.4974	1.4973
2	7114.90	7151.87	1.0801	1.0807	1.5788	1.5790
3	9793.24	9830.67	1.0530	1.0537	1.6520	1.6526
4	12 373.23	12 406.72	1.0315	1.0321	1.7212	1.7224
5	14 853.63	14 880.16	1.0136	1.0141	1.7887	1.7903
6	17 232.79	17 250.75	0.9983	0.9988	1.8555	1.8575
7	19 508.63	19 517.78	0.9851	0.9856	1.9228	1.9250
8	21 678.60	21 680.12	0.9735	0.9739	1.9912	1.9935
9	23 739.63	23 735.69	0.9633	0.9637	2.0617	2.0638
10	25 688.08	25 681.67	0.9543	0.9545	2.1350	2.1366
11	27 519.58	27 514.72	0.9462	0.9464	2.2122	2.2130
12	29 228.94	29 229.76	0.9391	0.9391	2.2947	2.2943
13	30 809.90	30 820.41	0.9328	0.9327	2.3840	2.3820
14	32 254.83	32 278.34	0.9272	0.9270	2.4825	2.4788
15	33 554.24	33 592.29	0.9224	0.9221	2.5939	2.5885
16	34 695.99	34 747.96	0.9183	0.9179	2.7242	2.7172
17	35 663.95	35 725.11	0.9149	0.9145	2.8843	2.8780

TABLE 5: Vibrational Levels of OCl($^2\Pi$)

v	V/cm^{-1}		$R_{\text{min}}/\text{\AA}$		$R_{\text{max}}/\text{\AA}$	
	calc.	exp.	calc.	exp.	calc.	exp.
0	420.35	425.68	1.5131	1.5131	1.6333	1.6334
1	1260.90	1268.47	1.4758	1.4758	1.6851	1.6854
2	2090.70	2100.11	1.4520	1.4521	1.7237	1.7241
3	2909.54	2920.5	1.4337	1.4338	1.7567	1.7574
4	3717.21	3729.5	1.4187	1.4187	1.7873	1.7878
5	4513.50	4527.0	1.4058	1.4058	1.8157	1.8163
6	5298.19	5312.9	1.3944	1.3945	1.8428	1.8435
7	6071.03	6086.9	1.3843	1.3844	1.8690	1.8697
8	6831.78	6849.1	1.3752	1.3752	1.8945	1.8952
9	7580.19	7599.3	1.3668	1.3669	1.9195	1.9202
10	8315.98		1.3592		1.9442	
11	9038.89		1.3521		1.9688	
12	9748.62		1.3455		1.9933	
13	10 444.86		1.3395		2.0178	
14	11 127.30		1.3338		2.0424	
15	11 795.61		1.3284		2.0671	
16	12 449.43		1.3234		2.0922	
17	13 088.40		1.3187		2.1175	

TABLE 6: Vibrational Levels of HCl ($^3\Sigma^+$)

v	V/cm^{-1}	$R_{\text{min}}/\text{\AA}$	$R_{\text{max}}/\text{\AA}$
0	17.6	3.5343	6.2051

TABLE 7: Vibrational Levels of OCl ($^2\Sigma^+$)

v	V/cm^{-1}	$R_{\text{min}}/\text{\AA}$	$R_{\text{max}}/\text{\AA}$
0	11.0	3.4298	4.1979
1	29.3	3.3070	4.7697
2	43.8	3.2464	5.3204
3	55.2	3.2090	5.9396
4	63.5	3.1854	6.7265
5	68.9	3.1712	7.8616
6	71.8	3.1639	9.7541
7	73.0	3.1610	13.7665

knowledge, no spectroscopic experimental information is available for the excited states investigated in the current work. Although the calculated values reported in Table 6 and Table 7 are very sensitive to small errors in the potential function (and hence should be viewed with some caution), they may be helpful to localize the corresponding spectral lines.

5. Conclusions

We have shown that the physically motivated EHFAC2(U) models are most adequate to describe the electronic states of HCl and OCl considered in the present work. To obtain the

fitting parameters when experimental data was unavailable, or else to test the theory, we have also reported accurate ab initio MRCI calculations for those electronic states by employing a full valence complete active space construction of the reference state and a large basis set (AVQZ). The calculated energies were then corrected through scaling of the external correlation to compensate for the truncation of the CI expansion and for the basis set incompleteness.

The model potential energy curves reported in the present work have shown high reliability when compared with the input data. Thus, they may be useful for molecular dynamics studies, particularly those referring to the photodissociation and predissociation of hypochlorous acid in ozone chemistry. The present study offers also a new test of the EHFAC2U model. The quality of the results achieved, together with the simplicity of the functional form, clearly recommend it to represent the two-body fragments of polyatomic potential-energy surfaces within the double many-body expansion method. In fact, this is currently being used to obtain a global two-valued potential energy surface for HOCl, with accurate ab initio electronic structure calculations at the levels reported in this work having already been completed. This ongoing work will hopefully be reported in a future publication.

Acknowledgment. A.P.G. thanks the Fundaci3n Gil D3vila, Spain, for a scholarship. This work has been supported by the Funda3o para a Ci4ncia e Tecnologia, Portugal, under program PRAXIS XXI.

References and Notes

- (1) Rowland, F. S.; Molina, M. J. *Rev. Geophys.* **1975**, *13*.
- (2) Warneck, P. *Z. Naturforsch.* **1977**, *32A*, 1254.
- (3) Solomon, S.; Garcia, R. R.; Rowland, F. S.; Waebbles, D. J. *Nature* **1986**, *321*, 755.
- (4) Barnes, R. J.; Dutton, G.; Sinha, A. J. *Phys. Chem.* **1997**, *101*, 8374.
- (5) Barnes, R. J.; Sinha, A. J. *Chem. Phys.* **1997**, *107*, 3730.
- (6) Wedlock, M. R.; Jost, R.; Rizzo, T. R. *J. Chem. Phys.* **1997**, *107*, 10 344.
- (7) Nanbu, S.; Iwata, S. *J. Phys. Chem.* **1992**, *96*, 2103.
- (8) S. Skokov, S. K. P.; Bowman, J. M. *J. Chem. Phys.* **1998**, *109*, 2662.
- (9) Hauschild, J.; Weiss, J.; Beck, C.; Grebenschikov, S. Y.; Dren, R.; Schinke, R.; Koput, J. *Chem. Phys. Lett.* **1999**, *300*, 569.
- (10) Horinek, D.; Dick, B. *Phys. Chem. Chem. Phys.* **1999**, *1*, 2667.
- (11) Vanderslice, J. T.; Mason, E. A.; Maisch, W. G.; Lippincott, E. R. *J. Mol. Spectrosc.* **1959**, *3*, 17.
- (12) Davies, M. R.; Shelley, J. C.; Roy, R. J. L. *J. Chem. Phys.* **1991**, *94*, 3479.
- (13) Varandas, A. J. C. *Adv. Chem. Phys.* **1988**, *74*, 255.
- (14) Varandas, A. J. C. *Dynamical Processes in Molecular Physics*; Delgado-Barrio, G., Ed.; IOP Publishing: Bristol, U.K., 1993; p 3.
- (15) Varandas, A. J. C.; Silva, J. D. *J. Chem. Soc., Faraday Trans. 2* **1986**, *82*, 593.
- (16) Varandas, A. J. C.; Nalewajski, R. F. *Chem. Phys. Lett.* **1993**, *205*, 253.
- (17) Varandas, A. J. C.; Silva, J. D. *J. Chem. Soc., Faraday Trans.* **1992**, *88*, 941.
- (18) Varandas, A. J. C.; Voronin, A. I. *Chem. Phys.* **1995**, *194*, 91.
- (19) Shavitt, I. *Advanced Theories and Computational Approaches to the Electronic Structure of Molecules*; Dykstra, C., Ed.; Reidel: Dordrecht, The Netherlands, 1984; p 185.
- (20) Werner, H.-J. *Adv. Chem. Phys.* **1987**, *67*, 1.
- (21) Roos, B. O.; Taylor, P. R.; Siegbahn, P. E. M. *Chem. Phys.* **1980**, *48*, 157.
- (22) Roos, B. O. *Adv. Chem. Phys.* **1987**, *69*, 399.
- (23) Brown, F. B.; Truhlar, D. G. *Chem. Phys. Lett.* **1985**, *117*, 307.
- (24) Varandas, A. J. C. *J. Chem. Phys.* **1989**, *90*, 4379.
- (25) Varandas, A. J. C. *J. Mol. Struct. Theochem.* **1985**, *120*, 401.
- (26) Varandas, A. J. C. *Mol. Phys.* **1987**, *60*, 527.
- (27) Roy, R. J. L. *Spec. Period. Rep. Chem. Soc. Mol. Spectrosc.* **1973**, *1*, 113.
- (28) Bunge, C. F.; Barrientos, J. A.; Bunge, A. V.; Cogordan, J. A. *At. Data Nucl. Data Tables* **1993**, *53*, 113.
- (29) Zeiss, G. D.; Meath, W. J. *Mol. Phys.* **1977**, *33*, 1155.

- (30) Chang, T. Y. *Rev. Mod. Phys.* **1967**, *39*, 911.
- (31) Werner, H.-J.; Knowles, P. J. *J. Chem. Phys.* **1988**, *89*, 5803.
- (32) Werner, H.; Knowles, P. J. *Chem. Phys. Lett.* **1988**, *145*, 514.
- (33) Werner, H.-J.; Knowles, P. J. *J. Chem. Phys.* **1985**, *82*, 5053.
- (34) Knowles, P. J.; Werner, H.-J. *Chem. Phys. Lett.* **1985**, *115*, 259.
- (35) Dunning, T. H. *J. Chem. Phys.* **1989**, *90*, 1007.
- (36) Kendall, R.; Dunning, T., Jr.; Harrison, R. *J. Chem. Phys.* **1992**, *96*, 6769.
- (37) Woon, D.; Dunning, T., Jr. *J. Chem. Phys.* **1993**, *98*, 1358.
- (38) MOLPRO is a package of ab initio programs written by H.-J. Werner and P. J. Knowles, with contributions from J. Almöf, R. D. Amos, A. Berning, M. J. O. Deegan, F. Eckert, S. T. Elbert, C. Hampel, R. Lindh, W. Meyer, A. Nicklass, K. Peterson, R. Pitzer, A. J. Stone, P. R. Taylor, M. E. Mura, P. Pulay, M. Schuetz, H. Stoll, T. Thorsteinsson, and D. L. Cooper, MOLPRO, 1996.
- (39) Sinanoğlu, O. *Adv. Chem. Phys.* **1964**, *6*, 315.
- (40) Silverstone, H. J.; Sinanoğlu, O. *J. Chem. Phys.* **1966**, *44*, 1899.
- (41) Öksüz, I.; Sinanoğlu, O. *J. Chem. Phys.* **1969**, *181*, 181.
- (42) Sinanoğlu, O.; Brueckner, K. A. *Three Approaches to Electron Correlation in Atoms*; Yale University: New Haven, CT, 1970.
- (43) Bauschlicher, C. W., Jr.; Walch, S. P.; Langhoff, S. R.; Taylor, P. R.; Jaffe, R. L. *J. Chem. Phys.* **1988**, *88*, 1743.
- (44) Steckler, R.; Schwenke, D. W.; Brown, F. B.; Truhlar, D. G. *Chem. Phys. Lett.* **1985**, *121*, 475.
- (45) Schwenke, D. W.; Steckler, R.; Brown, F. B.; Truhlar, D. G. *J. Chem. Phys.* **1986**, *84*, 5706.
- (46) Schwenke, D. W.; Steckler, R.; Brown, F. B.; Truhlar, D. G. *J. Chem. Phys.* **1987**, *86*, 2443.